Arh. farm. 2026; 76: 169 – 188 *Original scientific paper/Originalni naučni rad*

In Silico Evaluation of the Antibacterial and Antiviral Potential of Nusbiarylin Derivatives

Ognjen Milić[1], Nikola Nedeljković[2], Miloš Nikolić[2*]

[1]University of Belgrade – Faculty of Pharmacy, Department of Pharmaceutical Technology and Cosmetology, Vojvode Stepe 450, 11221 Belgrade, Serbia

[2]University of Kragujevac – Faculty of Medical Sciences, Department of Pharmacy, Svetozara Markovića 69, 34000 Kragujevac, Serbia

*Corresponding author: Miloš Nikolić, e-mail: milos.nikolic@fmn.kg.ac.rs

Received: 15 May 2026; Revised in revised forme: 16 June 2026; Accepted: 16 Jun 2026

Abstract

Antimicrobial resistance and chronic viral infections are major challenges in contemporary medicine. This *in silico* study evaluated the dual inhibitory potential of 16 designed nusbiarylin derivatives against two clinically relevant enzymatic targets: *Escherichia coli* (*E. coli)* RNA polymerase (RNAP) and hepatitis C virus RNA-dependent RNA polymerase (HCV RNAP). Semi-flexible molecular docking was performed using AutoDock Vina. Six compounds – 5, 6, 7, 8, 15, and 16 – showed the most favorable dual inhibitory potential, forming key hydrogen bonds with Ser642 of *E. coli* RNAP and with Tyr477 and Arg422 of HCV RNAP, along with significant hydrophobic interactions. The presence of cyano or nitroso groups as hydrogen bond acceptors, and sulfonyl or sulfoxide groups contributing π-S interactions, were identified as key determinants of binding affinity at both targets. These findings support further experimental evaluation of nusbiarylin derivatives as potential dual-activity antibacterial and antiviral agents.

Key words: molecular docking, nusbiarylin derivatives, drug-likeness analysis, RNA polymerase, HCV RNAP, dual inhibitors

https://doi.org/10.5937/arhfarm76-67266

Introduction

The emergence and rapid spread of antimicrobial resistance among clinically relevant pathogens is one of the most pressing challenges in contemporary medicine. The ongoing accumulation of resistance mechanisms has significantly narrowed the range of effective therapeutic options, especially for infections caused by multidrug-resistant bacterial strains and chronic viral infections (1). In this context, developing novel inhibitors that target essential microbial enzymes has become a priority in drug discovery, aiming to overcome existing resistance mechanisms and provide alternative therapeutic strategies (2).

Among the most extensively studied enzymatic targets are bacterial RNA polymerase (RNAP) and the RNA-dependent RNAP of hepatitis C virus (HCV RNAP). Both enzymes play central and indispensable roles in the replication of their respective pathogens and have structurally defined active sites that present well-characterized opportunities for pharmacological intervention. The nature of ligand-protein interactions at these sites – including hydrogen bond formation, hydrophobic interactions, and van der Waals contacts – determines the binding affinity of a compound and, consequently, its inhibitory potential (3, 4). A detailed understanding of these interactions is therefore essential for the rational design and optimization of new inhibitors. Identifying key amino acid residues involved in binding is particularly important, as specific interactions with these residues are critical for the inhibitory activity of small molecules against both *E. coli* RNAP and HCV RNAP (5, 6). Although approved inhibitors targeting both bacterial RNAP and HCV RNAP are available, the ongoing emergence of resistance necessitates the search for structurally novel compounds with distinct binding profiles. Ideally, compounds capable of inhibiting both targets simultaneously would be of considerable clinical interest, as they could broaden the spectrum of antimicrobial activity and reduce the likelihood of resistance development through target-specific mutations. Designing such dual-activity inhibitors requires thorough characterization of binding interactions at both enzymatic targets and careful evaluation of the structural requirements that govern productive engagement with each active site (7, 8).

Nusbiarylins are a class of diaryl molecules known to exert antibacterial activity by disrupting the NusB-NusE protein–protein interaction, a step essential for ribosomal RNA transcription (9). The present study was designed to assess whether nusbiarylin-based small molecules could also interact with enzymes involved in RNA transcription, specifically RNA polymerases of both bacterial and viral origin. Accordingly, 16 novel nusbiarylin derivatives were designed and further subjected to drug-likeness filtering to estimate their potential for favorable oral bioavailability and passive intestinal absorption. Subsequently, molecular docking was performed to investigate their binding interactions within the active sites of *E. coli* RNAP and HCV RNAP, with particular emphasis on binding free energy (docking scores), hydrogen bond formation, and the spatial orientation of key substituents within the binding pockets. *E. coli* RNAP was selected as a representative and well-characterized bacterial

transcriptional machinery, frequently used as a model system for the evaluation of antibacterial agents targeting transcription. In parallel, HCV RNAP was chosen as a clinically relevant and structurally well-defined RNA virus enzyme, recognized as a validated target in antiviral drug discovery and suitable for structure-based *in silico* studies due to the availability of high-resolution structural data.

Material and Methods

Drug-likeness Analysis

Empirical rules provide general criteria for identifying substances with greater potential as drug candidates. Drug-likeness analyses were conducted to determine, based on calculated molecular descriptors, whether a substance warrants further investigation. Molecular descriptors used in Lipinski's rule (10), Veber's rule (11), and Egan's rule (12) were calculated using Molinspiration Cheminformatics software, available online (13). Lipinski's rule includes the following molecular descriptors: molecular weight, hydrogen bond donors, hydrogen bond acceptors, and the logarithmic value of the octanol/water partition coefficient. Veber's rule considers structural parameters related to reduced molecular flexibility: the number of rotatable bonds and the polar surface area of the molecule. Additionally, the molecular formula and molecular volume were determined using ChemDraw Ultra 7.0 (14).

Selection and Preparation of Proteins

Three-dimensional crystallographic structures of the two target enzymes in complex with their respective co-crystallized ligands were retrieved from the Protein Data Bank (www.rcsb.org). The crystal structure of *E. coli* RNAP (PDB ID: 4ZH2) (15) in complex with a nusbiarylin derivative (N-hydroxy-N'-phenyl-3-(trifluoromethyl)benzenecarboximidamide, ligand ID: 4OB) and the crystal structure of the HCV RNA-dependent RNAP (PDB ID: 1YVX) (16) in complex with a nusbiarylin derivative (3-[isopropyl(4-methylbenzoyl)amino]-5-phenylthiophene-2-carboxylic acid, ligand ID: IPC) were selected as target models for this investigation. Prior to the docking procedure, co-crystallized ligands and solvent molecules were removed from the complete crystal structures using Discovery Studio 2017 (17). All docking calculations were performed on chains A and B of *E. coli* RNAP, as well as on chain A of HCV RNA-dependent RNAP. All co-crystallized ligands were removed from complete crystallographic structures or targeted proteins, retaining only the nusbiarylin derivative of interest.

Design and Preparation of Investigated Compounds

The structures of 16 nusbiarylin derivatives were drawn using ChemDraw Ultra 7.0. The design of these derivatives was based on the available structure-activity relationship (SAR) data for nusbiarylins reported in the literature (18, 19). The compounds were designed by structural modifications of the nusbiarylin scaffold, with particular attention to substituents on the disubstituted benzene ring and the nature of the linker connecting

the two aromatic systems, both of which have been identified as key determinants of binding affinity and antimicrobial activity. After structure drawing, all compounds were energy-minimized in Chem3D Ultra 7.0 (15) using the AM1 semiempirical method. The ligands were then processed in AutoDockTools 1.5.6 (20), where Gasteiger charges were assigned and torsional degrees of freedom specified.

Docking Methodology

Docking simulations were performed using AutoDock Vina (21) with its default scoring function under a semi-flexible protocol, in which the protein was kept rigid while the ligands were allowed rotational flexibility. The docking region was centered and defined based on the co-crystallized ligands binding site coordinates on *E. coli* and HCV RNAP with grid boxes of 26 × 22 × 28 and 22 × 20 × 32 points. Comparative analysis of the binding poses of nusbiarylin co-crystallized ligands and designed derivatives was conducted to assess their binding potential toward target proteins. The top-ranked binding poses, corresponding to the lowest binding energies (i.e. docking scores), were further examined within the enzyme's active site, and their interactions were visualized using Discovery Studio. Molecular docking was employed to characterize the nature and types of key non-covalent interactions, quantify their overall number, and evaluate binding affinities through docking scores.

Results

Design of Investigated Molecules

The design of the nusbiarylin derivatives (Figure 1) was carried out based on the available SAR data reported in the literature (18, 19).

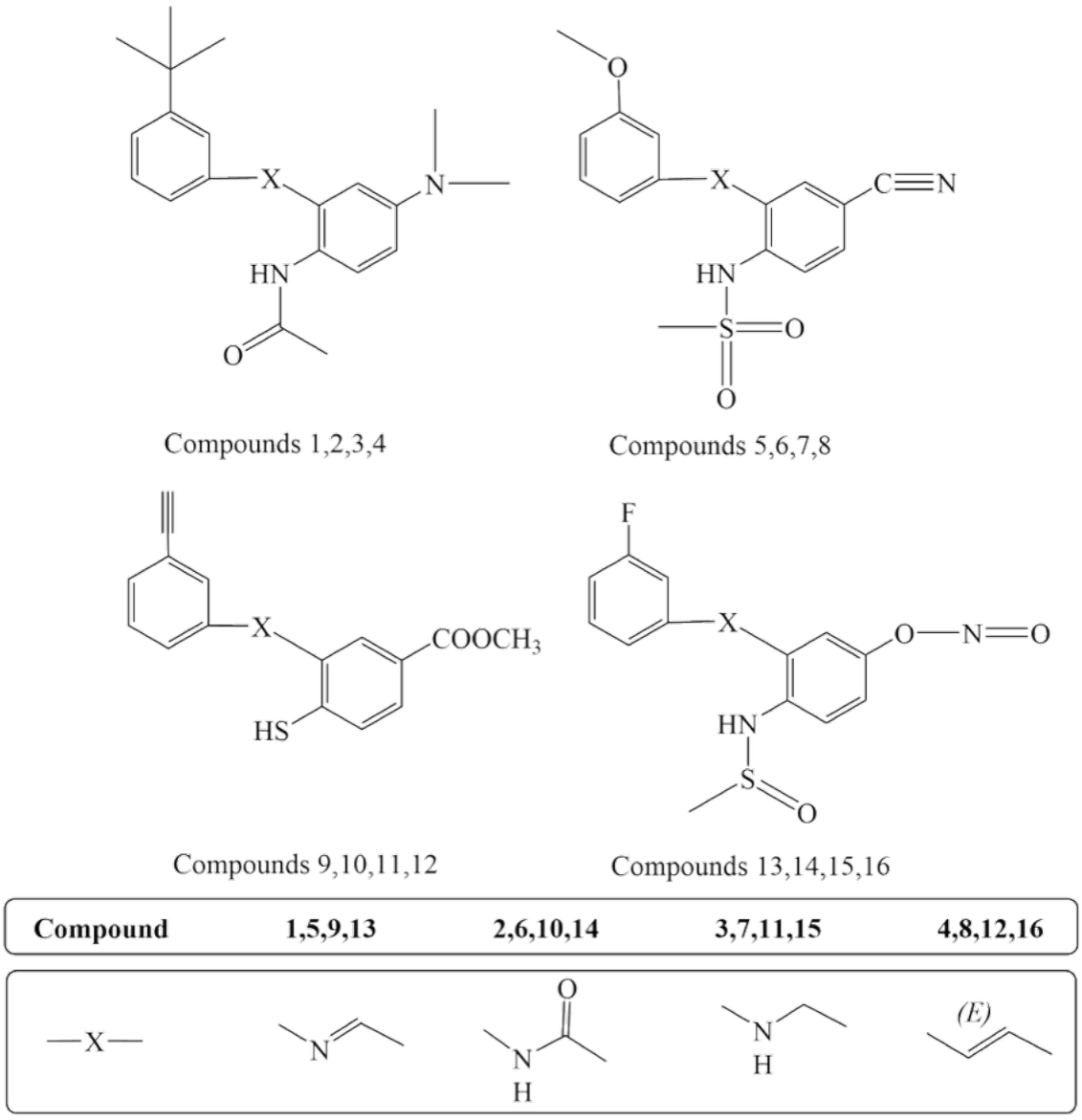

Figure 1. The chemical structures of the designed compounds (1–16)
Slika 1. Hemijska struktura dizajniranih jedinjenja (1–16)

Drug-likeness Analysis of the Designed Compounds

The data in Table I clearly show that all designed compounds, except compound 4, comply with all three rules – Lipinski's Rule of Five, Veber's rule, and Egan's rule – without significant deviations. Namely, none of the compounds exceed the Lipinski threshold for molecular weight (MW < 500 g/mol), hydrogen bond donors (nOHNH ≤ 5), or hydrogen bond acceptors (nON ≤ 10). Furthermore, all compounds satisfy Veber's criteria (nrotb ≤ 10 and TPSA ≤ 140 Å²) and Egan's criteria (miLogP ≤ 5.88 and TPSA ≤ 131.6 Å²).

Table I Physicochemical properties of the designed compounds used for the evaluation of drug-likeness rules

Tabela I Fizičko-hemijske osobine dizajniranih jedinjenja korišćene za procenu drug-likeness pravila

Compound	MF	MW (g/mol)	miLogP	nON	nOHNH	nrotb	TPSA (Å^2)	Volume (Å^3)	Nviolations
1	$C_{15}H_{13}F_3N_2O_3S$	378.33	3.62	6	2	6	96.40	312.97	0
2	$C_{15}H_{13}F_3N_2O_3S$	378.33	3.62	6	2	6	96.40	312.97	0
3	$C_{16}H_{15}F_3N_2O_3S$	392.36	3.97	6	2	7	96.40	332.11	0
4	$C_{17}H_{17}F_3N_2O_3S$	406.38	**4.32**	6	2	8	96.40	351.25	**1***
5	$C_{15}H_{12}F_3N_3O_2S$	371.33	3.19	7	1	6	105.63	308.65	0
6	$C_{16}H_{14}F_3N_3O_2S$	385.36	3.54	7	1	7	105.63	327.79	0
7	$C_{15}H_{12}F_3N_3O_2S$	371.33	3.19	7	1	6	105.63	308.65	0
8	$C_{16}H_{14}F_3N_3O_2S$	385.36	3.54	7	1	7	105.63	327.79	0
9	$C_{15}H_{13}F_3N_2O_4S$	394.33	3.13	7	2	6	113.33	321.97	0
10	$C_{16}H_{15}F_3N_2O_4S$	408.35	3.48	7	2	7	113.33	341.11	0
11	$C_{15}H_{12}F_3N_3O_3S$	387.33	2.70	8	1	6	122.57	317.65	0
12	$C_{16}H_{14}F_3N_3O_3S$	401.35	3.05	8	1	7	122.57	336.79	0
13	$C_{14}H_{11}F_4N_3OS$	361.31	3.26	6	1	5	87.43	293.65	0
14	$C_{15}H_{13}F_4N_3OS$	375.33	3.61	6	1	6	87.43	312.79	0
15	$C_{14}H_{10}F_4N_4O_2S$	390.31	2.83	8	1	5	113.47	306.22	0
16	$C_{15}H_{12}F_4N_4O_2S$	404.33	3.18	8	1	6	113.47	325.36	0

miLogP – partition coefficient; MW – molecular weight; MF – molecular formula; nrotb – number of rotatable bonds; volume – molecular volume; TPSA – topological polar surface area; nON – total number of hydrogen bond acceptors; nOHNH – total number of hydrogen bond donors; Nviolations – number of rule violations

* Value bolded indicates a violation of Lipinski's rule (miLogP > 4.15)

Compound 4 deviates from one rule: it has a miLogP value greater than 4.15, which violates Lipinski's Rule of Five. Specifically, its calculated miLogP is 4.32, exceeding the accepted threshold of 4.15, suggesting potentially reduced passive gastrointestinal absorption compared to the other designed molecules. The remaining compounds meet the criteria set by Lipinski's, Veber's, and Egan's rules, indicating favorable predicted oral bioavailability and passive intestinal absorption.

Validation of Docking Protocol

The docking protocol was validated through re-docking of each co-crystallized ligand into the binding site of its respective target protein. The accuracy of the procedure was evaluated by comparing the predicted binding pose with the experimentally resolved co-crystal structure, using the root-mean-square deviation (RMSD) as a metric. An RMSD value below 2 Å is generally indicative of a reliable docking setup. In this study, the RMSD values were 1.1983 Å for the *E. coli* RNAP ligand and 0.4128 Å (Figure 2A) for the HCV RNA-dependent RNAP, thereby supporting the accuracy of the applied docking methodology (Figure 2B).

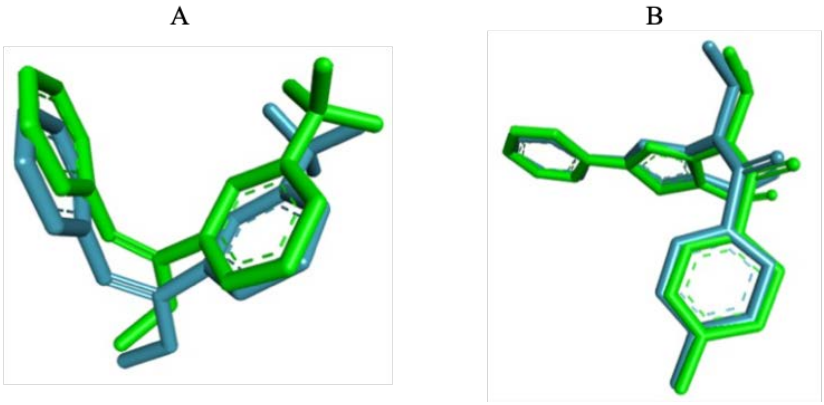

Figure 2. RMSD of the superimposed native and re-docked conformations of the co-crystallized ligand in *E. coli* RNAP (A) and HCV RNAP (B); the crystallographic poses are highlighted in light green, while the re-docked conformations are highlighted in dark green

Slika 2. RMSD preklopljene nativne i re-dokovane konformacije ko-kristalnog liganda u RNAP *E. coli* (A) i RNAP HCV (B); kristalografske poze su označene svetlo zelenom bojom, dok su redokovane konformacije označene tamno zelenom bojom

Binding Analysis

In this *in silico* study, 16 designed compounds were docked into the active site of the *E. coli* and HCV RNAP. In the interpretation of the molecular docking results, we considered the key binding interactions to be those interactions formed by the co-crystallized ligand during its molecular fitting into the active site of the targeted proteins. The category, type, total number of significant binding non-covalent interactions and docking scores of the best fitted ligand's poses are the main binding parameters of the tested compounds used to determine their binding analogy with the co-crystallized ligand's binding mode.

Based on the molecular docking results and obtained docking scores, it is evident that six compounds (compounds 5, 6, 7, 8, 15, and 16) formed the most stable ligand-receptor complexes (Table II). Furthermore, these compounds demonstrated comparable inhibitory capacity against both *E. coli* and HCV RNAP, while establishing interaction patterns similar to those observed for the corresponding co-crystallized ligands.

Table II The main molecular docking parameters of the designed compounds

Tabela II Glavni parametri molekulskog dokinga dizajniranih jedinjenja

Compound	*E. Coli* RNAP		HCV RNAP	
	Docking score	**Number of key binding interactions**	**Docking score**	**Number of key binding interactions**
1	–6.7	6	–7.6	4
2	–8.0	4	–7.7	5
3	–8.6	6	–6.8	6
4	–7.5	5	–7.8	2
5	–7.8	9	–8.2	5
6	–8.6	7	–7.5	5
7	–6.9	7	–8.0	5
8	–7.5	7	–8.3	5
9	–7.8	5	–8.0	5
10	–8.2	6	–8.0	6
11	–8.3	7	–7.2	6
12	–7.9	5	–7.9	5
13	–7.8	5	–7.6	5
14	–7.6	7	–7.5	5
15	–8.0	7	–7.4	5
16	–7.5	7	–7.7	5
Co-crystallized ligand	–9.2	-	–7.6	-

Compound 5

Molecular docking analysis of compound 5 revealed nine key binding interactions within the active site of *E. coli* RNAP. A single conventional hydrogen bond is formed between the nitrogen atom of the cyano group and Ser642 (hydrogen bond acceptor, bond length 2.23 Å). Hydrophobic interactions are formed with residues Ile774 (π-alkyl) and Ile755 (π-alkyl). Additionally, the oxygen atom of the sulfonyl group forms a non-conventional C-H hydrogen bond with Pro750, while the sulfur atom of the same moiety establishes a π-alkyl interaction with Phe773 (Figure 3A). On the other hand, five significant interactions are observed in the molecular interaction between compound 5 and HCV RNAP. Two hydrogen bonds are formed, one between the nitrogen of the cyano group and Tyr477 (hydrogen bond acceptor, bond length 2.69 Å), and another with Arg422, along with a C-H hydrogen bond established with Ile419. The remaining

interactions involve residues His475 (π-π) and Trp528 (π-π), while a π-S interaction is formed between the phenyl group of the designed molecule and the sulfur atom of the side chain of Met423 (Figure 3B).

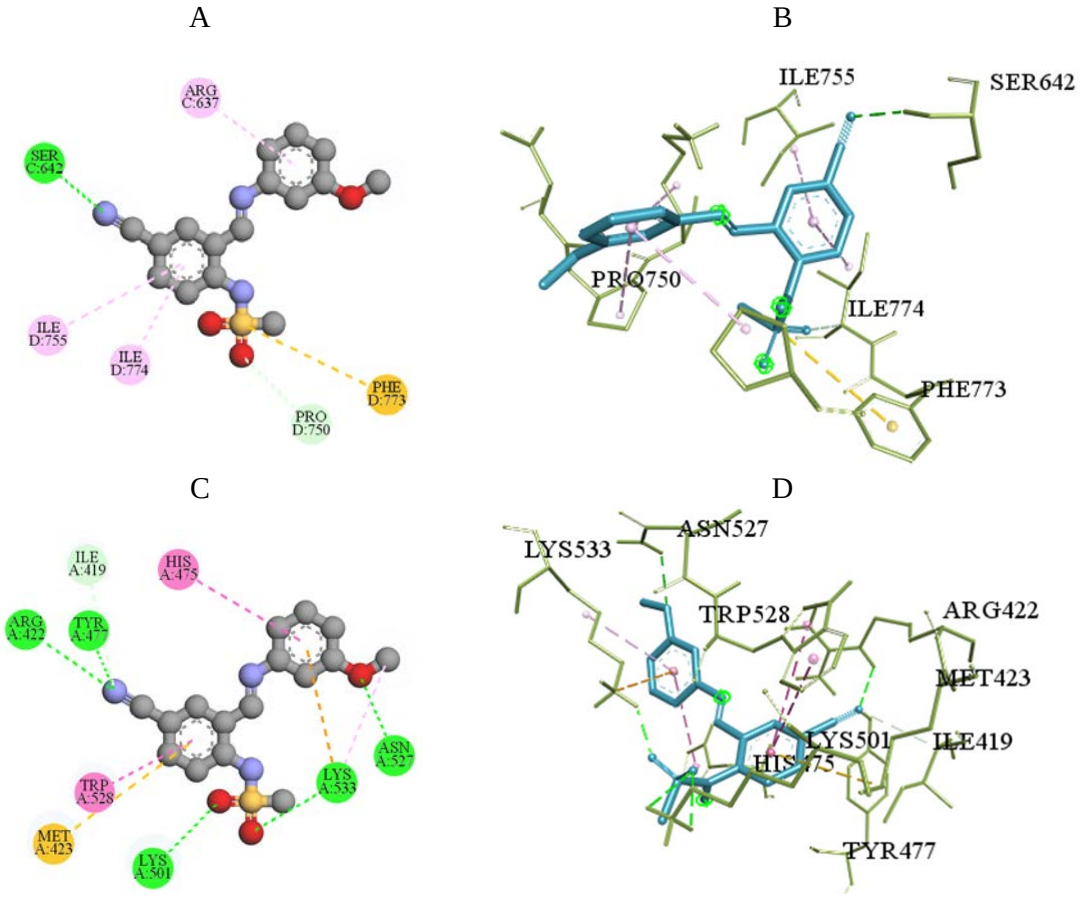

Figure 3. A two-dimensional and three-dimensional overview of the key binding interactions formed by compound 5 into the active site of *E. coli* RNAP (A and B) and HCV RNAP (C and D); conventional hydrogen bonds (green dotted lines), hydrophobic interactions (rose pink and magenta dotted lines), C-H hydrogen bonds (pale green dotted lines), and π-sulfur interactions (orange dotted lines) are shown

Slika 3. Predstavljen je dvodimenzionalni i trodimenzionalni prikaz ključnih interakcija koje jedinjenje 5 ostvaruje u aktivnom mestu RNAP *E. coli* (A i B) i RNAP HCV (C i D); klasične vodonične veze označene su zelenim isprekidanim linijama, hidrofobne interakcije ružičastim i ljubičastim isprekidanim linijama, C-H vodonične veze svetlo zelenim isprekidanim linijama, a π-sumporne interakcije narandžastim isprekidanim linijama

Compound 6

During molecular docking, compound 6 establishes seven key binding interactions within the active site of *E. coli* RNAP. Hydrophobic interactions are predominant, whereby four contacts are formed with the following amino acid residues: Ile755 (π-

alkyl), Ile774 (π-alkyl), Arg637 (π-alkyl), and Gly640 (amide-π). Hydrogen bonds are formed between the nitrogen atom of the cyano group of the designed molecule and Ser642 (hydrogen bond acceptor, bond length 2.30 Å), as well as between the sulfonyl moiety and Pro750 (C-H hydrogen bond). Among the additional significant binding interactions, the contact between the sulfonyl group and Phe773 (π-S) should also be noted (Figure 4A). Conversely, five significant interactions are observed in the molecular interaction between compound 6 and HCV RNAP (Figure 4B). Two hydrogen bonds are formed, one between the cyano group attached to the benzene ring and Tyr477 (hydrogen bond acceptor, bond length 2.65 Å), and another between Leu474 and the amide group connecting the two aromatic systems. The remaining three interactions involve residues His475 (π-π), as well as Met423 and Trp528 (van der Waals contacts).

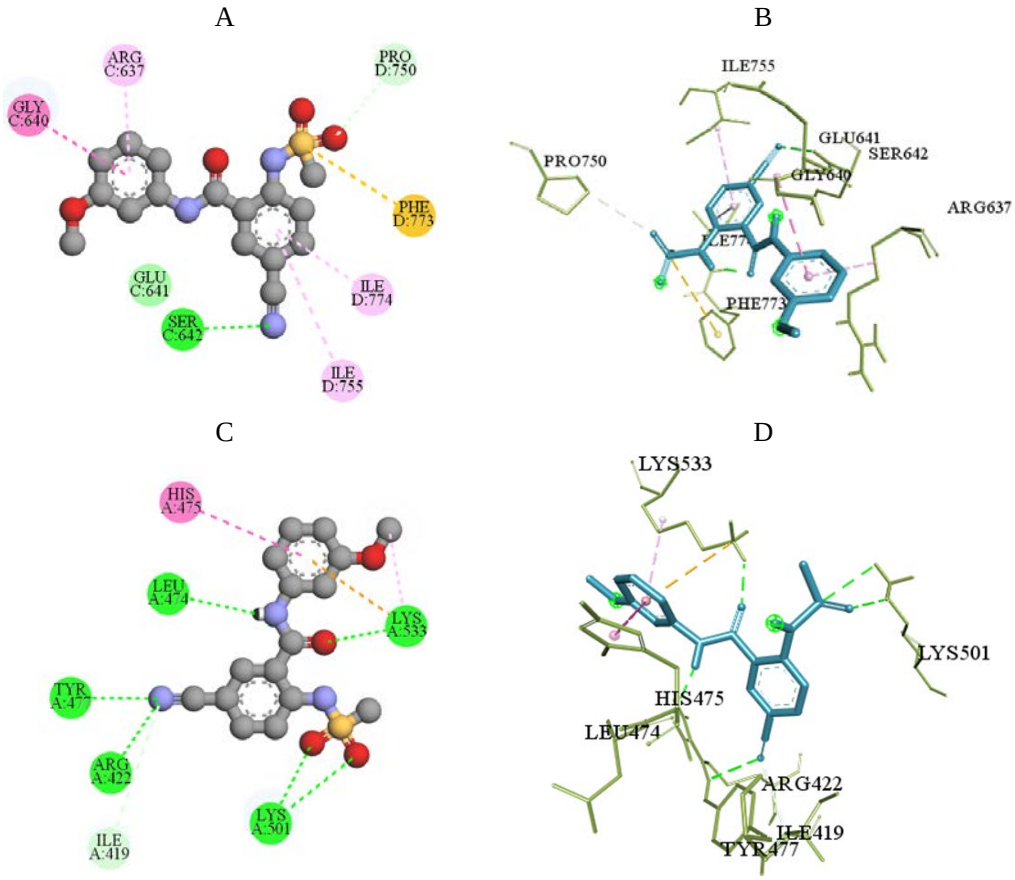

Figure 4. **A two-dimensional and three-dimensional overview of the key binding interactions formed by compound 6 into the active site of E. coli RNAP (A and B) and HCV RNAP (C and D); conventional hydrogen bonds (green dotted lines), hydrophobic interactions (rose pink and magenta dotted lines), and π-sulfur interactions (orange dotted lines) are shown**

Slika 4. **Predstavljen je dvodimenzionalni i trodimenzionalni prikaz ključnih interakcija koje jedinjenje 6 ostvaruje u aktivnom mestu RNAP E. coli (A i B) i RNAP HCV (C i D); klasične vodonične veze označene su zelenim isprekidanim linijama, hidrofobne interakcije ružičastim i ljubičastim isprekidanim linijama, a π-sumporne interakcije narandžastim isprekidanim linijama**

Compound 7

Upon binding of compound **7** to the active site of *E. coli* RNAP, seven key binding interactions are established. Residues Lys749 and Pro750 form van der Waals contacts, while residues Pro552 and Ile755 establish π-alkyl hydrophobic interactions. A conventional hydrogen bond is formed between the cyano group and Ser642 (hydrogen bond acceptor, bond length 2.05 Å), whereas Ile774 forms a C-H hydrogen bond. Among the remaining significant interactions, the contact between the oxygen of the sulfonyl group and Phe773 (π-S) should also be underlined (Figure 5A). In comparison, the

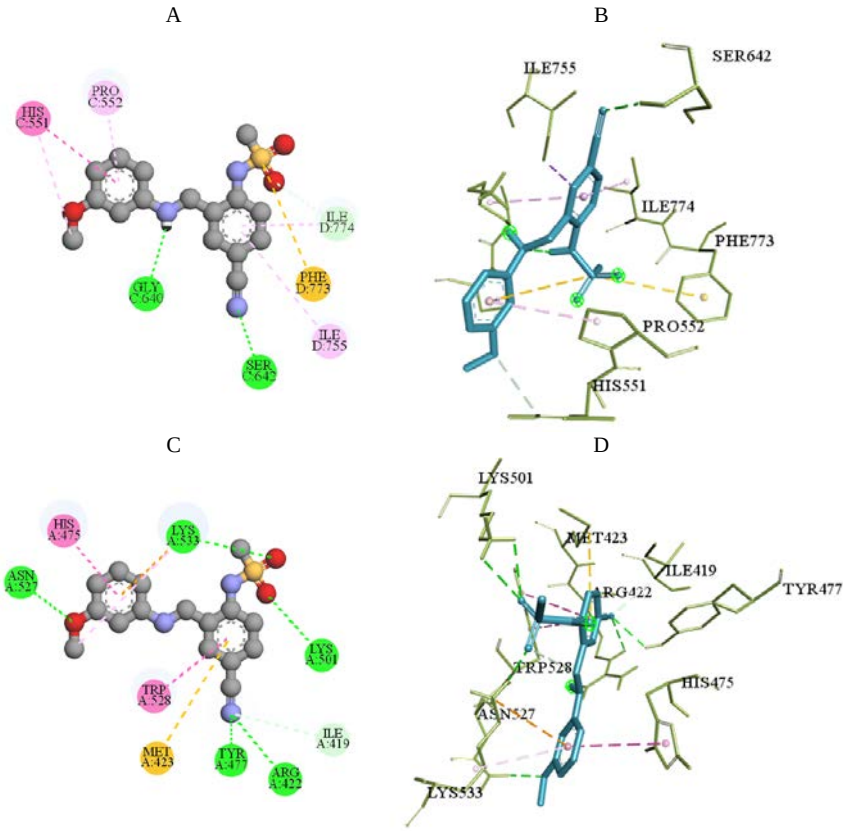

Figure 5. **A two-dimensional and three-dimensional overview of the key binding interactions formed by compound 7 into the active site of E. coli RNAP (A and B) and HCV RNAP (C and D); conventional hydrogen bonds (green dotted lines), hydrophobic interactions (rose pink and magenta dotted lines), C-H hydrogen bonds (pale green dotted lines), and π-sulfur interactions (orange dotted lines) are shown**

Slika 5. **Predstavljen je dvodimenzionalni i trodimenzionalni prikaz ključnih interakcija koje jedinjenje 7 ostvaruje u aktivnom mestu RNAP E. coli (A i B) i RNAP HCV (C i D); predstavljen je trodimenzionalni prikaz ključnih interakcija koje jedinjenje 7 ostvaruje pri vezivanju; klasične vodonične veze označene su zelenim isprekidanim linijama, hidrofobne interakcije ružičastim i ljubičastim isprekidanim linijama, C-H vodonične veze svetlo zelenim isprekidanim linijama, a π-sumporne interakcije narandžastim isprekidanim linijama**

molecular interaction of compound **7** with HCV RNAP is characterized by five binding contacts. π-π stacking contacts are formed with residues His475 and Trp528. Two hydrogen bonds are also observed, one between the phenyl ring and Tyr477 and another with Arg422, while an additional π-S interaction is formed between the benzene ring and Met423 (Figure 5B).

Compound 8

When docked into the active site of *E. coli* RNAP, compound 8 establishes seven key binding interactions. A single hydrogen bond is formed between the sulfonyl moiety of the designed molecule and Ser642 (hydrogen bond acceptor, bond length 2.61 Å). The remaining six interactions involving Pro552 (π-alkyl) and Ile774 (π-alkyl), whereas Ile755, Lys749, Pro552, and Phe773 engage through van der Waals contacts (Figure 6A).

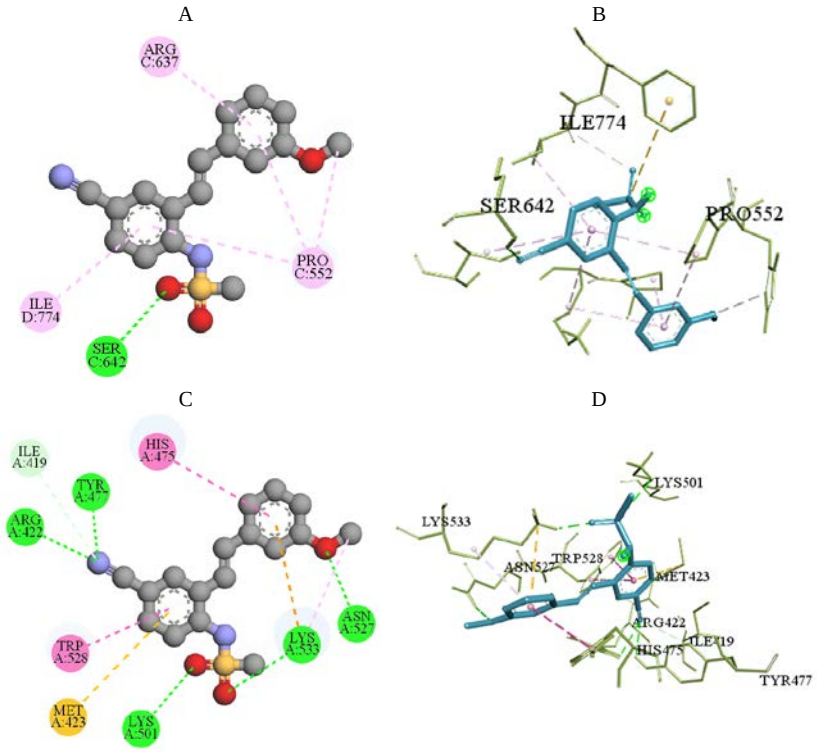

Figure 6. A two-dimensional and three-dimensional overview of the key binding interactions formed by compound 8 into the active site of *E. coli* RNAP (A and B) and HCV RNAP (C and D); conventional hydrogen bonds (green dotted lines), hydrophobic interactions (rose pink and magenta dotted lines), and π-sulfur interactions (orange dotted lines) are shown

Slika 6. Predstavljen je dvodimenzionalni i trodimenzionalni prikaz ključnih interakcija koje jedinjenje 8 ostvaruje u aktivnom mestu RNAP *E. coli* (A i B) i RNAP HCV (C i D); klasične vodonične veze označene su zelenim isprekidanim linijama, hidrofobne interakcije ružičastim i ljubičastim isprekidanim linijama, a π-sumporne interakcije narandžastim isprekidanim linijama

Conversely, the interaction of compound 8 with HCV RNAP involves five significant binding contacts. Two hydrogen bonds are formed, whereby the cyano group, Tyr477 and Arg422 are involved. Interaction between aromatic rings are observed with residues His475 (π-π) and Trp528 (π-π), while the benzene ring forms a π-S interaction with Met423 (Figure 6B).

Compound 15

The docking simulation of compound 15 within the active site of *E. coli* RNAP identified seven key binding interactions. The fluorine atom forms a C-H hydrogen bond with residue Lys649. Two conventional hydrogen bonds are also formed: one between the nitroso group directly attached to the phenyl ring and Pro552, and another between the sulfoxide moiety and Ser642 (hydrogen bond acceptor, bond length 2.97 Å). Hydrophobic interactions are established with Phe773 (π-π), Ile774 (π-alkyl), and Pro750 (π-alkyl). Attractive contacts additionally arise between the positively charged sulfur atom of the sulfonyl group and the negatively charged carboxylate of the Glu641 side chain (Figure 7A). On the other hand, five significant binding interactions are observed during molecular fitting of compound 15 within HCV RNAP active site. Three hydrogen bonds are formed: two involving the nitroso group with Tyr477 (hydrogen bond acceptor, bond length 2.36 Å) and Arg422, and a third between the amide group and Trp528. A single van der Waals contact is established with residue His475 (van der Waals), whereas the benzene ring forms a π-S interaction with Met423 (Figure 7B).

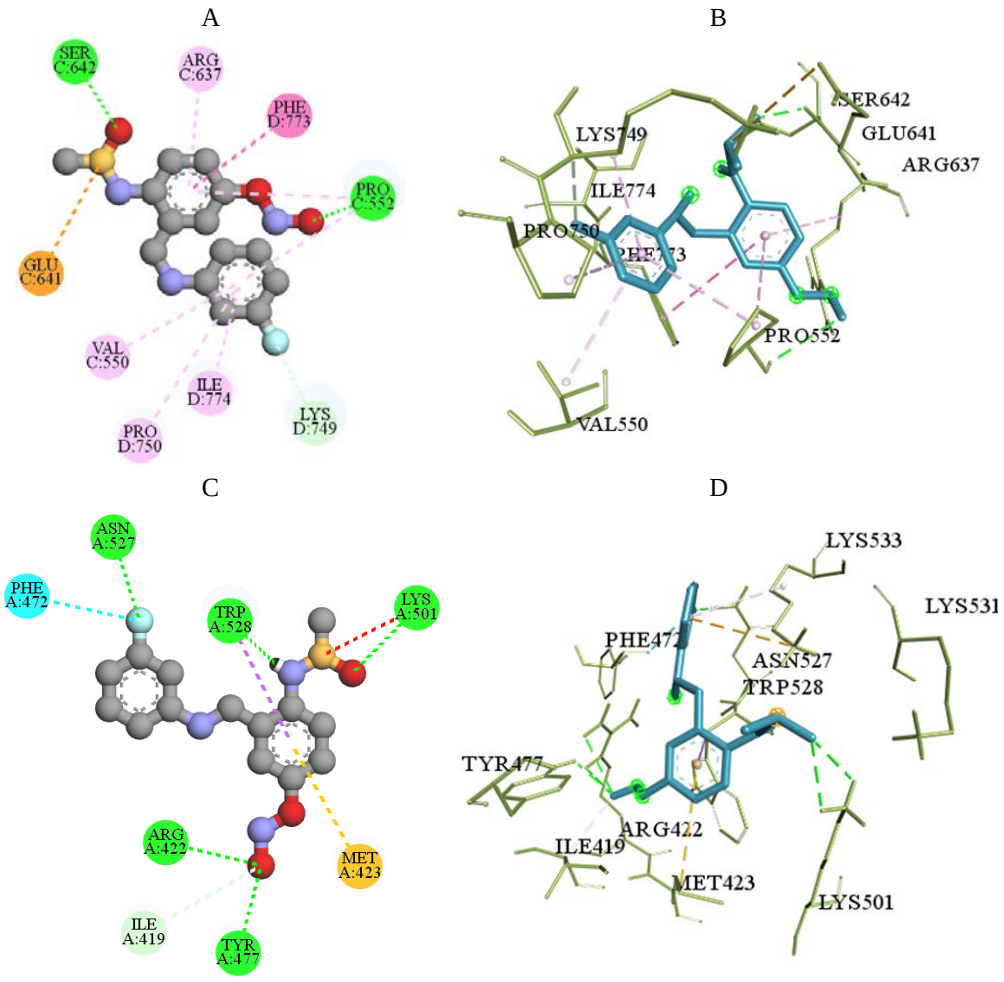

Figure 7. **A two-dimensional and three-dimensional overview of the key binding interactions formed by compound 15 into the active site of *E. coli* RNAP (A and B) and HCV RNAP (C and D); conventional hydrogen bonds (green dotted lines), C-H hydrogen bonds (pale green dotted lines), hydrophobic interactions (rose pink and magenta dotted lines), halogen interactions (cyan dotted lines), and electrostatic interactions (orange dotted lines) are shown**

Slika 7. **Predstavljen je dvodimenzionalni i trodimenzionalni prikaz ključnih interakcija koje jedinjenje 15 ostvaruje u aktivnom mestu RNAP *E. coli* (A i B) i RNAP HCV (C i D); konvencionalne vodonične veze označene su zelenim isprekidanim linijama, C-H vodonične veze svetlo zelenim isprekidanim linijama, hidrofobne interakcije ružičastim i ljubičastim isprekidanim linijama, halogenske interakcije tirkiznim isprekidanim linijama, a elektrostatičke interakcije narandžastim isprekidanim linijama**

Compound 16

Compound 16 establishes seven key binding interactions within the active site of *E. coli* RNAP. Hydrophobic interactions are predominant, with five contacts formed involving Ile755 (π-alkyl), Ile774 (π-alkyl), Lys749 (π-alkyl), Pro552 (amide-π), and Pro750 (π-alkyl). A hydrogen bond is formed between the nitrogen atom of the nitroso

group and Ser642 (hydrogen bond acceptor, bond length 2.03 Å). Among the additional significant binding interactions, the contact between the sulfoxide moiety and Phe773 (π-S) should also be highlighted (Figure 8A). Five key binding interactions are observed during the molecular docking of compound 16 in the HCV RNAP active site. Three hydrogen bonds are formed: two between the nitroso group attached to the benzene ring and Tyr477 (hydrogen bond acceptor, bond length 2.38 Å) and Arg422, respectively. A third hydrogen bond is formed between the secondary amino group of designed molecule and residue Trp528. His475 forms a π-π stacking interaction with the phenyl moiety of the designed compound, whereas the side chain of fMet423 establishes a π-S interaction with a second phenyl moiety (Figure 8B).

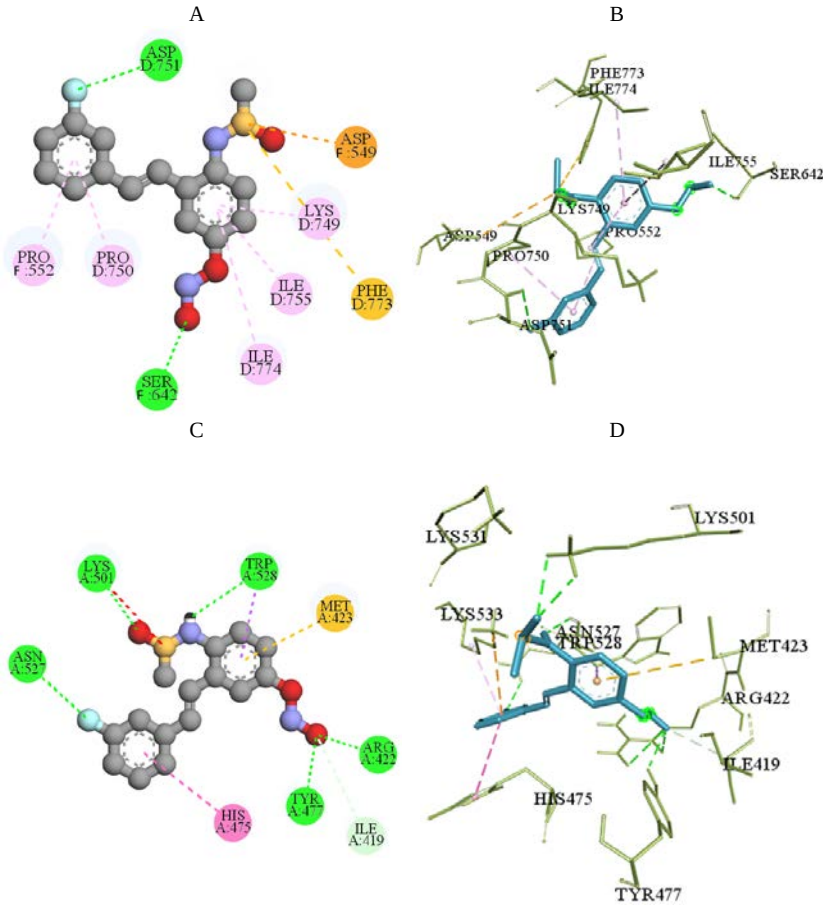

Figure 8. **A two-dimensional and three-dimensional overview of the key binding interactions formed by compound 16 into the active site of *E. coli* RNAP (A and B) and HCV RNAP (C and D); conventional hydrogen bonds (green dotted lines), hydrophobic interactions (rose pink and magenta dotted lines), electrostatic and π-sulfur interactions (orange dotted lines) are shown**

Slika 8. **Predstavljen je dvodimenzionalni i trodimenzionalni prikaz ključnih interakcija koje jedinjenje 16 ostvaruje u aktivnom mestu RNAP *E. coli* (A i B) i RNAP HCV (C i D); konvencionalne vodonične veze označene su zelenim isprekidanim linijama, hidrofobne interakcije ružičastim i ljubičastim isprekidanim linijama, a elektrostatičke i π-sumporne interakcije narandžastim isprekidanim linijama**

Discussion

The present *in silico* study first subjected designed nusbiarylin derivatives to drug-likeness analysis to evaluate their potential for favorable oral bioavailability and passive intestinal absorption, followed by an assessment of their binding affinity toward *E. coli* and HCV RNAP using molecular docking approach. Nusbiarylins are a novel class of diaryl compounds that exert antibacterial activity by indirectly inhibiting bacterial RNAP through disruption of the NusB-NusE protein-protein interaction, an essential step in ribosomal RNA transcription (9, 18). Building on the established structural scaffold and available SAR data, new derivatives were designed to identify compounds capable of simultaneously inhibiting both target enzymes.

For *E. coli* RNAP, none of the designed compounds achieved a docking score lower than that of the co-crystallized ligand. However, the differences were not substantial, and compound 6 came closest, with a value of –8.6 kcal/mol. For HCV RNAP, all compounds except compound 15 exhibited higher values of docking scores than the co-crystallized ligand, with compound 8 showing the lowest value of –8.3 kcal/mol. These findings indicate that while the designed compounds do not surpass the co-crystallized ligands in binding potential, their binding capacity is sufficiently favorable to warrant further experimental studies.

The key binding interactions identified in this study are consistent with those reported in related investigations. Bae et al. (6) examined the molecular docking of CBR inhibitors into *E. coli* RNAP using a model derived from comparative homology modeling and reported hydrogen bond formation with Ser642 and hydrophobic contacts with Ile774 and Pro552, the same interactions observed for the six best-performing compounds in this study. Similarly, Wang et al. (22) investigated the dual inhibitory potential of small molecules against HCV NS5B polymerase and reported that the benzene ring of the tested compounds formed hydrophobic interactions with Arg422, while the polar carboxyl group formed a conventional hydrogen bond with the main chain amide nitrogen of Tyr477, interactions also observed for compounds 15 and 16 in this study.

Analysis of the structural determinants of binding activity revealed that the presence of two aromatic benzene rings is essential for productive interaction with both target enzymes, with each ring contributing to binding through hydrogen bond formation or hydrophobic contacts. This finding is consistent with the SAR analysis reported by Qiu et al. (18), which demonstrated that the diaryl scaffold of nusbiarylins is a prerequisite for antimicrobial activity. Furthermore, in agreement with the same study, all six best-performing compounds contain a linker between the two aromatic systems consisting of at least two atoms, one of which is nitrogen, a structural feature identified as critical for optimal binding distance and orientation.

The nature of the substituents on the benzene rings was also an important determinant of binding. Compounds 5, 6, 7, and 8 contain a cyano group that serves as the primary hydrogen bond acceptor at both enzymatic targets, forming hydrogen bonds

with Ser642 in *E. coli* RNAP and with Tyr477 and Arg422 in HCV RNAP. Compounds 15 and 16 perform the same through a nitroso group, forming hydrogen bonds with the same key residues. The sulfonyl and sulfoxide groups in these compounds also contribute to binding through π-S interactions with Phe773 in *E. coli* RNAP and with Met423 in HCV RNAP. Notably, compound 15 was the only compound to form electrostatic interactions between the positively charged sulfur of the sulfonyl group and the negatively charged carboxyl side chain of Glu641 within *E. coli* RNAP active site, which may contribute to the stability of the ligand-receptor complex.

Conclusion

The results of this *in silico* molecular docking study show that compounds 5, 6, 7, 8, 15, and 16 were identified as the most promising candidates based on their lowest values of docking scores and the highest number of significant binding interactions with both target active sites. These six compounds reproduced the key binding contacts established by the respective co-crystallized ligands, including hydrogen bond formation with Ser642 in *E. coli* RNAP and with Tyr477 and Arg422 in HCV RNAP, as well as hydrophobic interactions with Ile774 and Pro552 in *E. coli* RNAP and with His475, Trp528, and Met423 in HCV RNAP.

Structural analysis of the best-performing compounds confirmed that two aromatic systems connected by a linker of at least two atoms are essential for dual inhibitory activity. The heteroaromatic ring present in the HCV RNAP co-crystal ligand was not required for productive binding, as compounds lacking a heteroaromatic system achieved comparable interaction profiles. The nature and position of substituents, particularly cyano and nitroso groups capable of hydrogen bond formation, and sulfonyl or sulfoxide groups contributing π-S interactions, were identified as key structural features governing binding at both targets.

These findings support the potential of nusbiarylin derivatives as a structural framework for developing dual-activity antibacterial and antiviral agents. Among the six designed compounds exhibiting the highest dual potential, compounds 15 and 16 can be highlighted, as they contain key structural determinants necessary for molecular interaction with the target proteins, making them promising candidates for future synthesis and biological evaluation.

Several limitations of the present study should be emphasized. The semi-flexible docking protocol assumes conformational rigidity of protein residues, representing another constraint of this work. Furthermore, the *in silico* analysis did not account for the role of water molecules within the active sites of the target proteins, which is a common limitation in molecular docking studies. To address this limitation, future research should include molecular dynamics simulations. Experimental validation through *in vitro* and *in vivo* studies will be required to confirm the antimicrobial and antiviral activities of the selected compounds.

Declaration of Competing Interest

The authors declare that they have no conflicts of interest to disclose, including financial, personal or other relationships.

Funding

The research was supported by the Ministry of Science, Technological Development and Innovation, Republic of Serbia, through Grant Agreements with the University of Belgrade – Faculty of Pharmacy (No 451-03-33/2026-03/200161 and No 451-03-34/2026-03/200161) and with Faculty of Medical Sciences, University of Kragujevac (No 451-03-34/2026-03/200111).

Author Contributions

O.M.: data curation, formal analysis, funding acquisition, investigation, methodology, resources, software, validation, writing – original draft, and writing – review & editing; **N.N.**: supervision, validation, and writing – review & editing. **M.N.**: conceptualization, funding acquisition, software, supervision, visualization, writing – original draft, and writing – review & editing.

All authors have read and agreed to the published version of the manuscript.

Data Availability Statement

The data that support the findings of this study are available from the corresponding author Miloš Nikolić upon reasonable request.

References

1. Allocati N, Masulli M, Alexeyev MF, Di Ilio C. Escherichia coli in Europe: An Overview. Int J Environ Res Public Health. 2013;10(12):6235–54.
2. Graham CS, Swan T. A path to eradication of hepatitis C in low- and middle-income countries. Antiviral Res. 2015;119:89–96.
3. Waheed Y, Bhatti A, Ashraf M. RNA dependent RNA polymerase of HCV: a potential target for the development of antiviral drugs. Infect Genet Evol. 2013;14:247–57.
4. Sutherland C, Murakami KS. An Introduction to the Structure and Function of the Catalytic Core Enzyme of Escherichia coli RNA Polymerase. EcoSal Plus. 2018;8(1). doi: 10.1128/ecosalplus.ESP-0004-2018.
5. Sesmero E, Thorpe IF. Using the Hepatitis C Virus RNA-Dependent RNA Polymerase as a Model to Understand Viral Polymerase Structure, Function and Dynamics. Viruses. 2015;7(7):3974–94.
6. Bae B, Nayak D, Ray A, Mustaev A, Landick R, Darst SA. CBR antimicrobials inhibit RNA polymerase via at least two bridge-helix cap-mediated effects on nucleotide addition. Proc Natl Acad Sci U S A. 2015;112(31):E4178–87.

7. Wei Y, Li J, Qing J, Huang M, Wu M, Gao F, et al. Discovery of Novel Hepatitis C Virus NS5B Polymerase Inhibitors by Combining Random Forest, Multiple e-Pharmacophore Modeling and Docking. PLoS One. 2016;11(2):e0148181.
8. Selami E, Berivan S, Yusuf S. Dual inhibitor design for HIV-1 reverse transcriptase and integrase enzymes: a molecular docking study. J Biomol Struct Dyn. 2020;38(2):573–80.
9. Yang X, Luo MJ, Yeung ACM, Lewis PJ, Chan PKS, Ip M, et al. First-In-Class Inhibitor of Ribosomal RNA Synthesis with Antimicrobial Activity against Staphylococcus aureus. Biochemistry. 2017;56(38):5049–52.
10. Lipinski CA, Lombardo F, Dominy BW, Feeney PJ. Experimental and computational approaches to estimate solubility and permeability in drug discovery and development settings. Adv Drug Deliv Rev. 2001;46(1–3):3–26.
11. Veber DF, Johnson SR, Cheng HY, Smith BR, Ward KW, Kopple KD. Molecular properties that influence the oral bioavailability of drug candidates. J Med Chem. 2002;45(12):2615–23.
12. Egan WJ, Merz KM Jr, Baldwin JJ. Prediction of drug absorption using multivariate statistics. J Med Chem. 2000;43:3867–77.
13. Molinspiration Cheminformatics [Internet]. Molinspiration; 2026 [cited 2026 April 18]. Available from: https://www.molinspiration.com/cgi-bin/properties.
14. Buntrock RE. ChemOffice Ultra 7.0. J Chem Inf Comput Sci. 2002;42(6):1505–6.
15. Feng Y, Degen D, Wang X, Gigliotti M, Liu S, Zhang Y, et al. Structural Basis of Transcription Inhibition by CBR Hydroxamidines and CBR Pyrazoles. Structure. 2015;23(8):1470–81.
16. Biswal BK, Cherney MM, Wang M, Chan L, Yannopoulos CG, Bilimoria D, et al. Crystal Structures of the RNA-dependent RNAP Genotype 2a of Hepatitis C Virus Reveal Two Conformations and Suggest Mechanisms of Inhibition by Non-nucleoside Inhibitors. J Biol Chem. 2005;280(18):18202–10.
17. Discovery Studio Visualizer. Version 17.2. [Internet]. Dassault Systèmes; 2016 [cited 2026 May 13]. Available from: https://www.3ds.com/products/biovia/discovery-studio/.
18. Qiu Y, Chan ST, Lin L, Shek TL, Tsang TF, Zhang Y, et al. Nusbiarylins, a new class of antimicrobial agents: Rational design of bacterial transcription inhibitors targeting the interaction between the NusB and NusE proteins. Bioorg Chem. 2019;92:103203.
19. Qiu Y, Chu AJ, Tsang TF, Zheng Y, Lam NM, Li KSL, et al. Synthesis and biological evaluation of nusbiarylin derivatives as bacterial rRNA synthesis inhibitor with potent antimicrobial activity against MRSA and VRSA. Bioorg Chem. 2022;124:105863.
20. Morris GM, Huey R, Lindstrom W, Sanner MF, Belew RK, Goodsell DS, et al. AutoDock4 and AutoDockTools4: Automated docking with selective receptor flexibility. J Comput Chem. 2009;30(16):2785–91.
21. Trott O, Olson AJ. AutoDock Vina: improving the speed and accuracy of docking with a new scoring function, efficient optimization, and multithreading. J Comput Chem. 2010;31(2):455–61.
22. Wang M, Ng KKS, Cherney MM, Chan L, Yannopoulos CG, Bedard J, et al. Non-nucleoside analogue inhibitors bind to an allosteric site on HCV NS5B polymerase: crystal structures and mechanism of inhibition. J Biol Chem. 2003;278(18):16149–58.

In silico ispitivanje antibakterijskog i antivirusnog potencijala derivata nusbiarilina

Ognjen Milić[1], Nikola Nedeljković[2], Miloš Nikolić[2*]

[1]Univerzitet u Beogradu – Farmaceutski fakultet, Katedra za farmaceutsku tehnologiju i kozmetologiju, Vojvode Stepe 450, 11221 Beograd, Srbija

[2]Univerzitet u Kragujevcu – Fakultet medicinskih nauka, Odsek za farmaciju, Svetozara Markovića 69, 34000 Kragujevac, Srbija

*Autor za korespondenciju: Miloš Nikolić, e-mail: milos.nikolic@fmn.kg.ac.rs

Kratak sadržaj

Antimikrobna rezistencija i hronične virusne infekcije predstavljaju značajne izazove u savremenoj medicini. U ovoj *in silico* studiji ispitivan je dualni inhibitorni potencijal 16 dizajniranih derivata nusbiarilina prema dva klinički relevantna enzimska cilja: RNK polimerazi bakterije *Escherichia coli* (*E. coli*) (RNAP) i RNK-zavisnoj RNK polimerazi virusa hepatitisa C (HCV RNAP). Semifleksibilno molekulsko doking ispitivanje sprovedeno je korišćenjem softvera AutoDock Vina. Šest jedinjenja – 5, 6, 7, 8, 15 i 16 – pokazala su najpovoljniji dualni inhibitorni potencijal, formirajući ključne vodonične veze sa Ser642 *E. coli* RNAP i sa Tyr477 i Arg422 HCV RNAP, uz značajne hidrofobne interakcije. Prisustvo cijano ili nitrozo grupa kao akceptora vodoničnih veza, kao i sulfonil ili sulfoksidnih grupa koje doprinose π-S interakcijama, identifikovano je kao ključna strukturna determinanta afiniteta vezivanja za oba ciljna mesta. Ovi rezultati podržavaju dalje eksperimentalno ispitivanje derivata nusbiarilina kao potencijalnih dualnih antibakterijskih i antivirusnih agenasa.

Ključne reči: molekulski doking, derivati nusbiarilina, analiza sličnosti sa lekom, RNK polimeraza, HCV RNAP, dualni inhibitori